Journal of Alloys and Compounds 509 (2011) 6908–6912

Contents lists available at ScienceDirect

Journal of Alloys and Compounds

journal homepage: www.elsevier.com/locate/jallcom

Crystal structure and microwave dielectric properties of $ZnTi(Nb_{1-x}Ta_x)_2O_8$ ceramics

Jeong-Hyun Park[a,b], Young-Jin Choi[a], Sahn Nahm[b], Jae-Gwan Park[a,*]

[a] Nano-Photonics Research Center, Korea Institute of Science and Technology, Seoul 136-791, Republic of Korea
[b] Department of Materials Science and Engineering, Korea University, Seoul 136-701, Republic of Korea

ARTICLE INFO

Article history:
Received 22 November 2010
Received in revised form 18 March 2011
Accepted 30 March 2011
Available online 6 April 2011

Keywords:
Ceramics
Crystal structure
X-ray diffraction
TEM

ABSTRACT

The crystal structure and microwave dielectric properties of $ZnTi(Nb_{1-x}Ta_x)_2O_8$ ($0 \le x \le 1$) ceramics sintered at 1200 °C for 2 h were investigated. For $x < 0.5$, solid solution phases with the α-PbO_2 structure, typical of $ZnTiNb_2O_8$, were obtained, whereas for $0.5 \le x < 1$, mixtures of two solid solutions each respectively based on the α-PbO_2 structure and a trirutile structure, were obtained. The relative amount of the trirutile-structured phases increased as the Ta content increased in a given region, and the end member $ZnTiTa_2O_8$ formed a single phase with the trirutile structure. The microwave dielectric properties were closely related to the crystal structures. A material with a near zero temperature coefficient of resonant frequency could be obtained for $x = 0.8$, and its dielectric constant and quality factor ($Q \times f$) were 40.5 and 41,000 GHz, respectively.

© 2011 Elsevier B.V. All rights reserved.

1. Introduction

The rapid growth of satellite and personal mobile communications has resulted in the need for narrow band, temperature-stable materials that operate at high frequencies. In recent decades, microwave dielectric ceramic materials have been investigated for use in wireless communication components, such as duplexers, resonators, antennas, and oscillators. To utilize these at high frequencies, low-loss materials with moderate dielectric constant (k) characteristics and near-zero temperature coefficients of resonant frequency (τ_f) are required [1–3].

In this regard, AB_2O_6 (A = Mg, Zn, Ca, Co, Ni, Cu, Mn; B = Nb, Ta) compounds have attracted great attention due to their promising microwave dielectric properties [4–6]. The greater part of these compounds may largely be classified into two structural groups, that is, trirutile-type tetragonal and columbite-type orthorhombic structures [4,16–18], and their microwave dielectric properties have been found to be strongly dependent on the structure type along as well as on the chemical composition [4,18]. Recently, a number of studies have been conducted on $(A'_{1-y}A''_y)B_2O_6$- or $A(B'_{1-y}B''_y)_2O_6$-type material systems, in which the microwave dielectric properties were expected to be tunable by controlling the crystal phases by means of compositional variation [7–10,18]. In the $ZnNb_2O_6$–TiO_2 system, an ixiolite phase $ZnTiNb_2O_8$ with a fully disordered α-PbO_2 structure was first reported by Baumgarte and Blachnik [11,12], and its microwave dielectric properties were investigated by Kim et al. [13] and were reported as follows: k of 34.3, τ_f of −52 ppm/°C, and a quality factor of 42,500 GHz.

In this report, we investigated the $ZnTi(Nb_{1-x}Ta_x)_2O_8$ ($0 \le x \le 1$) system, focusing on the effect of substitution with Ta ions, which have greater ionicity and thus a stronger ordering tendency than Nb ions, on the crystal structural behavior. We also investigated the relationship between crystal structures and microwave dielectric properties in the system, expecting that the greater ionicity of the Ta ions could increase not only the dielectric constant to a moderate value, but also would cause τ_f to reach a near zero value for use in practical microwave component applications.

2. Experimental

$ZnTi(Nb_{1-x}Ta_x)_2O_8$ ($0 \le x \le 1$) ceramics were prepared by the conventional solid-state mixed oxide method, using high purity (>99.9%) powders of ZnO, Nb_2O_5, Ta_2O_5, and TiO_2 (High Purity Chemical Lab., Japan). The starting oxides were weighed in appropriate proportions for $x = 0$, 0.25, 0.5, 0.75, and 1, and mixed for 12 h in polyethylene bottles containing zirconia balls and ethanol. After drying the mixed slurry in an oven, the powders were calcined at 1050 °C for 3 h. The calcined powders were re-milled for 6 h. After drying, the powders were pressed uniaxially under 1000 kg/cm^2 into disk pellets with a diameter of 10 mm. The pellets were sintered in air at temperatures ranging from 1100 °C to 1250 °C for 2 h, in order to evaluate the densification behavior.

The bulk density of the sintered specimens was measured by the Archimedes method. The relative density was obtained from the theoretical density that was calculated from the lattice parameters determined by X-ray diffraction analysis. The crystal structures of the samples were characterized with an X-ray powder diffractometer (XRD, D8 Advance, Bruker, Karlsruhe, Germany) using CuK_α radiation and transmission electron microscopy (TEM, G2, Tecnai, Hong Kong). The sintered microstructure was examined by scanning electron microscopy (SEM, S-3000H, Hitachi, Tokyo, Japan). The local chemical composition was analyzed using

* Corresponding author. Tel.: +82 2 958 5503; fax: +82 2 958 5509.
E-mail address: jgpark@kist.re.kr (J.-G. Park).

0925-8388/$ – see front matter © 2011 Elsevier B.V. All rights reserved.
doi:10.1016/j.jallcom.2011.03.178

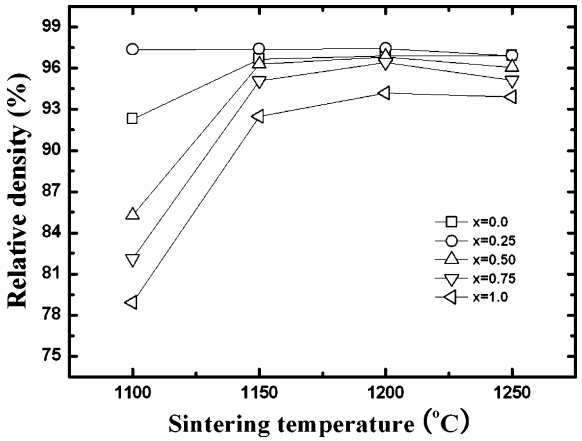

Fig. 1. The relative densities of $ZnTi(Nb_{1-x}Ta_x)_2O_8$ ceramics sintered at various temperatures for 2 h.

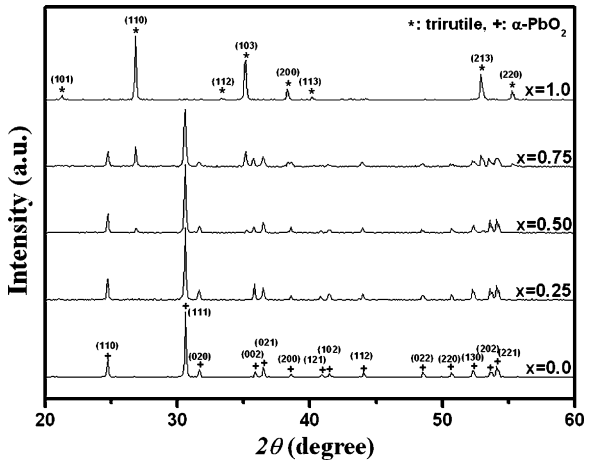

Fig. 3. XRD patterns of $ZnTi(Nb_{1-x}Ta_x)_2O_8$ ceramics sintered at 1200 °C for 2 h.

TEM energy-dispersive spectroscopy (EDS, ISIS 310, Oxford, UK) and an electron probe micro-analyzer (EPMA, JXA-8500F, JEOL, Tokyo, Japan).

The microwave dielectric properties of the sintered samples in the frequency range of 8–12 GHz were measured using a network analyzer (HP 8720 C, Hewlett-Packard, Palo Alto, USA). The dielectric constant was measured via the Hakki–Coleman post resonator method [14] by exciting the TE_{011} mode, and the quality factor was measured using the $TE_{01\delta}$ mode with the cavity method [15]. The temperature coefficient of the resonance frequency was calculated with the temperature variation of the $TE_{01\delta}$ mode in the range of 20–80 °C.

3. Results and discussions

Fig. 1 shows the temperature and compositional dependence of the relative density of $ZnTi(Nb_{1-x}Ta_x)_2O_8$ ceramics sintered at various temperatures ranging from 1100 °C to 1250 °C for 2 h. We can see that irrespective of their composition, all samples exhibited maximum densities at 1200 °C and they seemed to have been overfired at 1250 °C. By firing at 1200 °C, the highest density of about 98% of the theoretical density was attained for $x = 0.25$, whereas the sintered densities of the other compositions were in the range of about 94–97% and tended to decrease as x increased. Therefore, we focused mainly on the 1200 °C-2 h sintered samples for examining the structural and dielectric behaviors of the ceramics.

Fig. 2 illustrates back scattered SEM images of $ZnTi(Nb_{1-x}Ta_x)_2O_8$ ceramics for $x = 0.5$ and 0.75, which were sintered at 1200 °C for 2 h. We can see that the ceramics seemed to consist of two types of grains, bright grains and dark grains, indicating a possible coexistence of two types of crystal phases. It is noticeable that for $x = 0.75$, the dark grains were larger in size and quantity than those for $x = 0.5$. The Roman numbers given in the micrographs indicate the positions where the EPMA analysis was performed. The analysis result, which relates chemical composition to the darkness of grains, will be presented later, along with the TEM/EDS result.

Fig. 3 shows the XRD patterns of $ZnTi(Nb_{1-x}Ta_x)_2O_8$ ceramics sintered at 1200 °C for 2 h. By indexing the patterns, it becomes apparent that the system consists of two structural types, orthorhombic α-PbO_2 and tetragonal trirutile structures. For $x = 0$, the end member $ZnTiNb_2O_8$ (i.e. $ZnNb_2O_6$–TiO_2), formed a single phase with the α-PbO_2 structure, in which the cation-coordinating octahedra forms zig–zag chains by sharing skew edges, and the cations are fully disordered. This result is consistent with the report by Baumgarte and Blachnik [11], in which they described that $ZnTiNb_2O_8$ had an α-PbO_2 related ixiolite structure, which is a substructure of the columbite structure of $ZnNb_2O_6$. It is noteworthy that the TiO_2 destroys the 1:2 cation ordering, but maintains the skew-edge-shared zigzagged chain structure, in the columbite structure of $ZnNb_2O_6$.

On the other hand, for $x = 1$, the other end member, $ZnTiTa_2O_8$ (i.e. $ZnNb_2O_6$–TiO_2), formed a single phase and adopted the trirutile structure, in which the unit cell of rutile is triplicated in the c-axis direction. In the rutile structure, the edge-sharing octahedra chains are straight instead of zigzagged. The (1 0 1) and (1 1 2) peaks in the diffraction pattern confirm the trirutile structure and are kinds of superlattice diffraction peaks, which do not exist for the rutile structure. $ZnTa_2O_6$ is known to have a tri-α-PbO_2 structure [8], which is an ordered variant of the α-PbO_2 structure. It is worthy to note that in this case, the TiO_2 changes the tri-α-PbO_2 structure of the $ZnTa_2O_6$ with the zigzagged chains into a trirutile structure with straight chains.

For $x = 0.25$, the nominal composition $ZnTiNb_{1.5}Ta_{0.5}O_8$ resulted in a single-phase solid solution with an α-PbO_2 structure; the cations were randomly distributed in the skew-edge-shared oxygen octahedra. The same result was obtained for $x = 0.35$, though

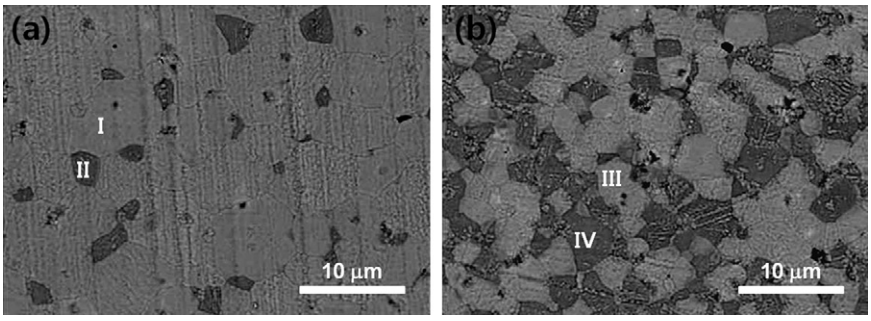

Fig. 2. The back scattered SEM micrograph of $ZnTi(Nb_{1-x}Ta_x)_2O_8$ ceramics sintered at 1200 °C for 2 h; (a) $x = 0.5$ and (b) $x = 0.75$.

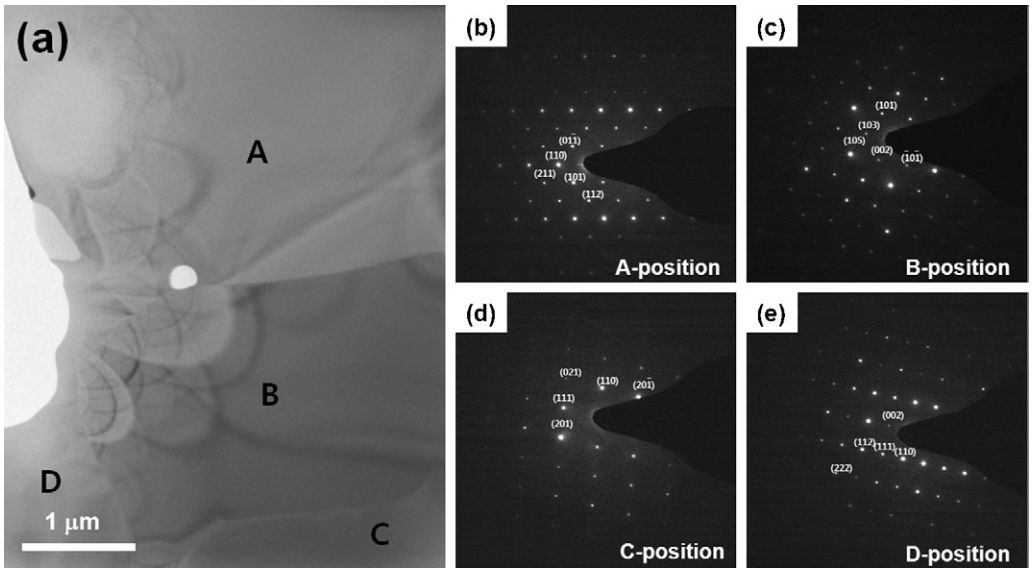

Fig. 4. (a) TEM bright field image of $ZnTi(Nb_{0.25}Ta_{0.75})_2O_8$ ceramics sintered at 1200 °C for 2 h; (b), (c), (d), and (e) are SAED patterns of positions A, B, C, and D, in (a), respectively.

the data is not presented here. It is likely that for roughly $x < 0.5$, single phases with the α-PbO_2 structure will form. However, for $x = 0.5$ and 0.75, the nominal compositions were $ZnTiNbTaO_8$ and $ZnTiNb_{0.5}Ta_{1.5}O_8$, respectively, and they did not form a single phase, but rather a mixture of two solid solution phases, that is, an α-PbO_2-structured phase and a trirutile-structured phase. Due to the low intensities of the latter, i.e. the minor phase, we were unable to discern whether it possessed the rutile structure or the trirutile structure base on the XRD patterns. However, using the TEM analyses presented later in this paper, it was confirmed that the phase had the trirutile structure. The relative amount of the trirutile-structured phase to the α-PbO_2-structured phase increased when x increased in the region $x \geq 0.5$.

This type of crystal structural behavior has been explained as the difference of the covalency (or iconicity) between Nb^{5+} and Ta^{5+} ions. It was pointed out that in various mixed metal oxides, Ta^{5+} ions are more ionically bonded than Nb^{5+} ions, and the tendency towards covalent bonding is greater for Nb^{5+} than for Ta^{5+} [16]. It was postulated that in the columbite (and its substructure, α-PbO_2) structure, there is bonding between metal ions, whereas in the trirutile structure, the pentavalent ions are far apart [16]. In general, in AB_2O_6-type oxides, Nb^{5+} ions with high covalency prefer the columbite structure, while Ta^{5+} ions with high ionicity favor the trirutile structure, with a few exceptions [10,16–19].

In order to investigate the exact crystal phases and to confirm the coexistence of the α-PbO_2 and trirutile phases in the mixture of the two solid solution phases, specimens of the $ZnTi(Nb_{1-x}Ta_x)_2O_8$ ceramics for $x = 0.75$ sintered at 1200 °C for 2 h were thinned by ion milling and analyzed by TEM. A typical TEM bright-field image is shown in Fig. 4a, revealing several grains. The selected area electron diffraction (SAED) patterns obtained for the four positions of A, B, C, and D in the bright field image are shown in Fig. 4b, c, d, and e, respectively. By indexing the SAED patterns, we confirmed that the two grains of the A and B positions have the trirutile structure, whereas those of C and D have the α-PbO_2 structure. The interplanar distances of the (1 0 1) plane in the patterns of the A and B positions were measured to be 4.15 Å and 4.12 Å, respectively. The (1 1 1) plane in the patterns for C and D positions had measured interplanar distances of 2.98 Å and 2.99 Å, respectively. We could not observe the rutile or columbite structure at all, even for different samples. Therefore, we concluded that the minor phase observed in the XRD patterns for $x = 0.5$ and 0.75 possessed the trirutile structure, not the disordered rutile structure.

Since there may be a certain relationship between structure type and chemical composition, we performed TEM/EDS analyses for the four positions in Fig. 4a, and the results are shown in Table 1. It is revealed that the positions with the trirutile structure have Ti/Zn and Ti/Nb ratios greater than normal stoichiometric ratios, whereas those with the α-PbO_2 structure have cation ratios smaller than normal ratios. In other words, the trirutile phase is Ti-rich and Zn–Nb-poor compared with the nominal composition, while the α-PbO_2 phase is Ti-poor and Zn–Nb-rich. The Ta content varies relatively little in the two crystal phases. Even though phase boundaries are not investigated in detail here and remain uncertain, it can be postulated that in the region $0.5 \leq x < 1$, $ZnTi(Nb_{1-x}Ta_x)_2O_8$ ceramics split into two solid solution phases, i.e. the Ti-rich trirutile-structured phase and the Zn–Nb-rich α-PbO_2-structured phase. It seems natural that the Ti-rich phase adopts the trirutile structure, while the Zn-Nb-rich phase possesses the $ZnNb_2O_6$-like α-PbO_2-structure, which is a disordered columbite structure. It is expected that there might be a saturated composition for both solid solution phases. Detailed study on the phase boundaries and saturated compositions is

Table 1
TEM EDS analysis result of $ZnTi(Nb_{0.25}Ta_{0.75})_2O_8$ ceramics marked in Fig. 4a.

Position	Zn	Ti	Nb	Ta	Ti/Nb	Ti/Zn	(Zn + Nb)/Ti	Crystal structure (at.%)
A	20.3	26.8	12.1	41.0	2.21 (2)*	1.32 (1)*	1.21 (1.5)*	Trirutile
B	23.7	27.4	12.8	39.5	2.14 (2)*	1.16 (1)*	1.33 (1.5)*	Trirutile
C	24.0	20.7	13.5	41.4	1.53 (2)*	0.87 (1)*	1.81 (1.5)*	α-PbO_2
D	23.2	18.5	13.6	42.7	1.36 (2)*	0.80 (1)*	1.99 (1.5)*	α-PbO_2

*The numbers in parentheses are nominal ratio.

Table 2
EPMA analysis result of $ZnTi(Nb_{1-x}Ta_x)_2O_8$ ceramics marked in Fig. 2.

	Position	Zn	Ti	Nb	Ta	Ti/Nb	Ti/Zn	(Zn + Nb)/Ti	Crystal structure	Grain color (at.%)
$x = 0.50$	I	25.7	23.2	25.5	25.6	0.90 (1)*	0.90 (1)*	2.20 (2.0)*	α-PbO_2	Grey
	II	23.4	32.6	21.3	22.7	1.53 (1)*	1.39 (1)*	1.37 (2.0)*	Trirutile	Dark grey
$x = 0.75$	III	25.8	20.4	16.5	37.3	1.23 (2)*	0.79 (1)*	2.07 (1.5)*	α-PbO_2	Grey
	IV	24.6	27.9	11.9	35.6	2.34 (2)*	1.13 (1)*	1.31 (1.5)*	Trirutile	Dark grey

*The numbers in parentheses are nominal ratio.

necessary to clarify the structural phase relationship of the system.

The EPMA analysis was performed for the four positions of I–IV in Fig. 2 for $ZnTi(Nb_{1-x}Ta_x)_2O_8$ ($x = 0.5, 0.75$) samples and the results are summarized in Table 2. Since the micrographs in Fig. 2 are back-scattered SEM images, phases with higher density that consisted of heavier elements are darker in the analysis compared to the phases that consisted of light elements. It was found that the chemical composition of bright grains is Ti-poor and Nb–Zn-rich compared with the nominal composition, whereas the chemical composition of dark grains is Ti-rich and Nb–Zn-poor. Considering the above TEM/EDS result, we can postulate that the bright grains represent the α-PbO_2-structured phase, and the dark ones represent the trirutile-structured phase. The increase in the amount of dark grains for $x = 0.75$ compared with that for $x = 0.5$ supports this postulation.

The microwave dielectric properties of the $ZnTi(Nb_{1-x}Ta_x)_2O_8$ ceramics sintered at 1200 °C for 2 h are shown in Figs. 5 and 6. For $x < 0.5$, where the ceramics were single phase solid solutions with an α-PbO_2 structure, their dielectric constant (k) and temperature coefficient of resonant frequency (τ_f) changed little, while the quality factor ($Q \times f$) had the highest value for $x = 0.25$. The high $Q \times f$ of this composition could be connected with its high sintered density and microstructural uniformity. For $x \geq 0.5$, where the ceramics consisted of mixtures of two solid solutions with α-PbO_2 and trirutile structures, k and τ_f increased when x increased, while $Q \times f$ decreased. This behavior can be explained by the fact that the relative amount of the trirutile-structured phase to the α-PbO_2-structured phase increased when x increased. The trirutile-structured phase seemed to exhibit TiO_2(rutile)-like dielectric behaviors, such as a high k and positive τ_f, while the α-PbO_2-structured phase seemed to exhibit $ZnNb_2O_6$(columbite)-like dielectric behaviors, such as a negative τ_f. It is expected that the τ_f could be near zero for $x = 0.8$. In this case, the ceramics had a k of 40.5 and $Q \times f$ of 41,000 GHz. The end member $ZnTiTa_2O_8$, which was confirmed to be a single phase with a trirutile structure, had a k of 47.1, $Q \times f$ of 35,800 GHz, and τ_f of +84 ppm/°C.

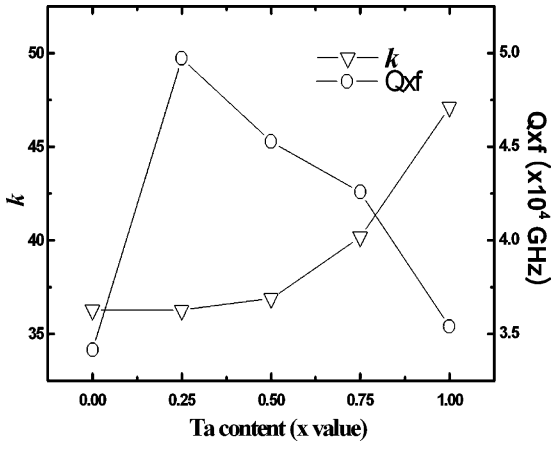

Fig. 5. Dielectric constant and quality factor of $ZnTi(Nb_{1-x}Ta_x)_2O_8$ ceramics sintered at 1200 °C for 2 h.

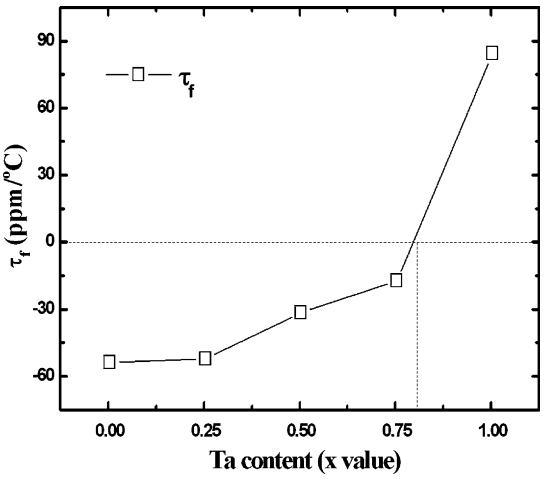

Fig. 6. Temperature coefficient of resonant frequency of $ZnTi(Nb_{1-x}Ta_x)_2O_8$ ceramics sintered at 1200 °C for 2 h.

4. Conclusion

The crystal structural changes and their effects on the microwave dielectric properties of $ZnTi(Nb_{1-x}Ta_x)_2O_8$ ($0 \leq x \leq 1$) ceramics sintered at 1200 °C for 2 h were investigated in this study. It was revealed that, while one end member, $ZnTiNb_2O_8$ ($x = 0$), possessed the α-PbO_2 structure, which is a fully disordered variant of the columbite structure, the other end member, $ZnTiTa_2O_8$ ($x = 1$), had an ordered trirutile structure. For $x < 0.5$, the solid solution phases possessed the α-PbO_2-structure only, whereas for $0.5 \leq x < 1$, two kinds of solid solutions, each respectively based on the α-PbO_2 structure and trirutile structure, coexisted as a mixture, and the relative amount of the trirutile phase increased as x increased. It was recognized that in the two-phase mixtures, the α-PbO_2 phase was relatively Ti-poor and Nb–Zn-rich, whereas in the trirutile phase, is the phase was relatively Ti-rich and Nb–Zn-poor compared to the nominal composition. The microwave dielectric properties of the $ZnTi(Nb_{1-x}Ta_x)_2O_8$ ceramics were closely related to the crystal structures: for $x < 0.5$, the ceramics with an α-PbO_2 structure exhibited columbite-like dielectric behavior, while for $x \geq 0.5$, the ceramics exhibited more rutile-like behaviors as x increased. The $ZnTiTa_2O_8$ ceramics were found to have a k of 47.1, $Q \times f$ of 35,800 GHz, and τ_f of +84 ppm/°C. A promising microwave dielectric material with a near zero τ_f could be obtained for $x = 0.8$, and its k and quality factor ($Q \times f$) were 40.5 and 41,000 GHz, respectively.

Acknowledgement

This research was supported by a grant from the Center for Advanced Materials Processing (CAMP) of the Knowledge Economy Frontier R&D Program funded by the Ministry of Knowledge Economy (MKE), Republic of Korea.

References

[1] H.W. Lee, J.H. Park, J.S. Nahm, D.W. Kim, J.G. Park, Mater. Res. Bull. 45 (2010) 21–24.
[2] H. Jantunen, R. Rautioaho, A. Unsimäki, S. Leppävuori, J. Eur. Ceram. Soc. 20 (2000) 2331–2336.
[3] L. Fang, Q. Yu, C. Hu, H. Zhang, Mater. Lett. 61 (2007) 4140–4143.
[4] H.J. Lee, I.T. Kim, K.S. Hong, Jpn. J. Appl. Phys. 36 (10A) (1997) 1318–1320.
[5] H.J. Lee, K.S. Hong, S.J. Kim, I.T. Kim, Mater. Res. Bull. 32 (7) (1997) 847–855.
[6] R.C. Pullar, J.D. Breeze, N.M. Alford, J. Am. Ceram. Soc. 88 (9) (2005) 2466–2471.
[7] C.L. Huang, J.Y. Chen, J. Am. Ceram. Soc. 93 (5) (2010) 1248–1251.
[8] Y.C. Zhang, Z.X. Yue, X. Qi, B. Li, Z. Gui, L. Li, Mater. Lett. 58 (2004) 1392–1395.
[9] C.L. Huang, J.Y. Chen, J. Am. Ceram. Soc. 93 (2) (2010) 470–473.
[10] W.C. Tzou, Y.C. Chen, C.F. Yang, C.M. Cheng, Mater. Res. Bull. 41 (2006) 1357–1363.
[11] A. Baumgarte, R. Blachnik, Mater. Res. Bull. 27 (1992) 1287–1294.
[12] A. Baumgarte, R. Blachnik, J. Alloys Compd. 210 (1994) 75–81.
[13] D.W. Kim, D.Y. Kim, K.S. Hong, J. Mater. Res. 15 (6) (2000) 1331–1335.
[14] B.W. Hakki, P.D. Coleman, IRE Trans. Microwave Theory Tech. 8 (1960) 402–410.
[15] D. Kaifez, P. Guillion, Dielectric Resonator, Artech House, Norwood, MA, 1986, pp. 327–376.
[16] G. Blasse, J. Inorg. Nucl. Chem. 26 (1964) 1191–1199.
[17] M. López-Blanco, U. Amador, F. García-Alvarato, J. Solid State Chem. 182 (2009) 1944–1949.
[18] M. Thirumal, A.K. Ganguli, Mater. Res. Bull. 36 (2001) 2421–2427.
[19] E.J. Felten, Mater. Res. Bull. 2 (1967) 13–24.